microbial biotechnology

Open Access

# The sulfur formation system mediating extracellular cysteine-cystine recycling in *Fervidobacterium islandicum* AW-1 is associated with keratin degradation

**Hyeon-Su Jin,[1,†] Immanuel Dhanasingh,[2,†] Jae-Yoon Sung,[1] Jae Won La,[1] Yena Lee,[1] Eun Mi Lee,[3] Yujin Kang,[4] Do Yup Lee,[3] Sung Haeng Lee[2] and Dong-Woo Lee[1]**

[1]*Department of Biotechnology, Yonsei University, Seoul, 03722, South Korea.*

[2]*Department of Cellular and Molecular Medicine, Chosun University School of Medicine, Gwangju, 61452, South Korea.*

[3]*Department of Agricultural Biotechnology, Center for Food and Bioconvergence, Research Institute for Agricultural and Life Sciences, Seoul National University, Seoul, 08826, South Korea.*

[4]*Department of Bio and Fermentation Convergence Technology, BK21 PLUS Program, Kookmin University, Seoul, 02707, Korea.*

## Summary

**Most extremophilic anaerobes possess a sulfur formation (Suf) system for Fe–S cluster biogenesis. In addition to its essential role in redox chemistry and stress responses of Fe–S cluster proteins, the Suf system may play an important role in keratin degradation by *Fervidobacterium islandicum* AW-1. Comparative genomics of the order Thermotogales revealed that the feather-degrading *F. islandicum* AW-1 has a complete Suf-like machinery (SufCBDSU) that is highly expressed in cells grown on native feathers in the absence of elemental sulfur ($S^0$). On the other hand, *F. islandicum* AW-1 exhibited a significant retardation in the Suf system-mediated keratin degradation in the presence of $S^0$. Detailed differential expression analysis of sulfur assimilation machineries unveiled the mechanism by which an efficient sulfur delivery from persulfurated SufS to SufU is achieved during keratinolysis under sulfur starvation. Indeed, addition of SufS–SufU to cell extracts containing keratinolytic proteases accelerated keratin decomposition *in vitro* under reducing conditions. Remarkably, mass spectrometric analysis of extracellular and intracellular levels of amino acids suggested that redox homeostasis within cells coupled to extracellular cysteine and cystine recycling might be a prerequisite for keratinolysis. Taken together, these results suggest that the Suf-like machinery including the SufS–SufU complex may contribute to sulfur availability for an extracellular reducing environment as well as intracellular redox homeostasis through cysteine released from keratin hydrolysate under starvation conditions.**

Received 9 September, 2020; revised 8 November, 2020; accepted 11 November, 2020.

For correspondence. E-mail leehicam@yonsei.ac.kr; Tel. +82-2-2123-2886; Fax +82-2-362-7265. sunglee@chosun.ac.kr; Tel: +82-62-230-6381; Tel: +82-62-608-5314

[†]These authors contributed equally to this work.

*Microbial Biotechnology* (2021) **14**(3), 938–952
doi:10.1111/1751-7915.13717

## Introduction

Iron–sulfur (Fe–S) clusters play a pivotal role in numerous cellular processes including respiration, photosynthesis and nitrogen fixation. Fe–S cluster-containing proteins are highly specific for sensing various redox signals including levels of oxidative stress and the abundance of elements such as iron, and they are involved in responses and adaptation to environmental changes, resulting in adaptive cellular responses (Mettert and Kiley, 2015; Golinelli-Cohen and Bouton, 2017). Sulfur is a vital element in all living cells for the biosynthesis of Fe–S clusters, sulfur-containing amino acids and vitamins, and RNA through a variety of modifications (Mueller, 2006). Its delivery to the Fe–S cluster biogenesis system is a sophisticated process. Elaborate sulfur transfer systems are widely distributed from bacteria to humans (Johnson *et al.*, 2005; Kessler, 2006; Mueller, 2006). Bacterial sulfur mobilization systems have diverged into three main distinct systems: (i) the iron-sulfur cluster (Isc) system (Zheng *et al.*, 1998; Py and Barras, 2010), (ii) the nitrogen fixation (Nif) system (Jacobson *et al.*, 1989; Zheng *et al.*, 1993) and (iii) the sulfur formation (Suf) system (Takahashi and Tokumoto, 2002; Ayala-Castro *et al.*, 2008; Vaccaro *et al.*, 2017).

The Suf system initially involves a cysteine desulfurase (SufS) and a sulfur acceptor protein (SufE), that mobilize and relay sulfur to SufBCD (Layer *et al.*, 2007). In the case of the U-type protein containing *suf*CDSUB gene cluster in the phylum Firmicutes, SufU accepts

© 2020 The Authors. *Microbial Biotechnology* published by Society for Applied Microbiology and John Wiley & Sons Ltd.
This is an open access article under the terms of the Creative Commons Attribution-NonCommercial-NoDerivs License, which permits use and distribution in any medium, provided the original work is properly cited, the use is non-commercial and no modifications or adaptations are made.

sulfur from SufS, but it remains elusive whether SufU acts as SufE, or as an Fe–S cluster biosynthetic scaffold (Fujishiro *et al*., 2017). SufS catalyses the pyridoxal-5'-phosphate (PLP)-dependent removal of sulfur from L-cysteine, yielding L-alanine and persulfide $S^0$ species *via* the formation of a protein-bound persulfide (R–S–SH) intermediate (Zheng *et al*., 1994; Schwartz *et al*., 2000; Mihara and Esaki, 2002). Subsequently, the protein persulfide group is transferred from SufS to SufE *via* a persulfide exchange reaction, thereby greatly increasing SufS activity (Layer *et al*., 2007; Roche *et al*., 2013). The reduced persulfide is incorporated into the Fe–S cluster as sulfide ($S^{2-}$) during assembly on the SufBCD complex as scaffold protein (Loiseau *et al*., 2003; Outten *et al*., 2003; Layer *et al*., 2007). These multi-step processes are required for Fe–S cluster and methionine biogenesis *in vivo* (Mueller, 2006, Dai and Outten, 2012). Due to the reactivity of both the persulfide intermediate and the sulfhydryl groups, Fe–S cluster assembly is prone to oxidative damage. Unlike the analogous Isc system, the Suf system is highly expressed upon exposure to oxidative stress or iron starvation (Outten *et al*., 2004; Huet *et al*., 2005; Shi *et al*., 2010; Marinoni *et al*., 2012). In general, primordial environments rich in iron and inorganic sulfur under anaerobic conditions might exert selective pressure and promote the evolution of several sulfur assimilation pathways including the Suf system for Fe–S cluster biogenesis (Rees and Howard, 2003; Py and Barras, 2010; Groussin and Gouy, 2011; Hidese *et al*., 2014; Vaccaro *et al*., 2017). Remarkably, SufS orthologs are widely distributed in many thermophilic bacteria and mesophilic archaea, but not in the most hyperthermophilic Crenarchaeotal genera such as *Sulfolobus* or *Pyrobaculum* (Liu *et al*., 2010). However, the hyperthermophilic Euryarchaeon *Thermococcus kodakarensis* contains a group II SufS that is only required for growth when $S^0$ is not available as a sulfur source (Hidese *et al*., 2014). Thus, among hyperthermophiles there are multiple and/or alternative pathways for maintaining Fe–S cluster biogenesis under different nutrient conditions.

The extremophilic bacterium *Fervidobacterium islandicum* AW-1, belonging to the order Thermotogales, can completely degrade insoluble feathers composed of β-keratins at 70°C under anaerobic conditions (Nam *et al*., 2002). This impressive capability is of special interest for agricultural, environmental and biomedical applications (Tsiroulnikov *et al*., 2004; Fosgerau and Hoffmann, 2015; Lange *et al*., 2016). Moreover, keratin degradation is of direct relevance for converting insoluble agro-waste into high-value products (Kang *et al*., 2020) and for providing insight into the pathogenesis of superficial infections by dermatophytes (Grumbt *et al*., 2013). However, the degradation mechanism of insoluble fibrous proteins rich in cysteine remains unclear. To gain mechanistic insight into feather degradation associated with Fe–S cluster biogenesis, the Suf system of *F. islandicum* AW-1 was phylogenetically and physicochemically characterized in detail. This comprehensive study led us to hypothesize the plausible role of the Suf system for keratin degradation. Indeed, together with growth profiles of *F. islandicum* AW-1 in the presence and absence of $S^0$, differential expression profiles of the genes involved in sulfur metabolism indicated that poor $S^0$ availability might necessitate the use of the Suf system responsible for extracellular reducing environments as well as intracellular redox homeostasis via a cysteine-cystine recycling. Therefore, these results suggest that the Suf-like machinery-mediated redox chemistry may promote cleavage of disulfide bonds in keratin (sulfitolysis) as well as the subsequent removal of sulfur from cysteine for Fe–S cluster biogenesis, resulting in accelerated decomposition of recalcitrant keratin polymers under starvation conditions.

## Results

### *The suf gene cluster is potentially associated with keratin degradation in Fervidobacteriaceae*

The 16S rRNA gene-based phylogenetic analysis of 20 representative bacterial strains of the order Thermotogales known to be related to *Fervidobacterium islandicum* AW-1 demonstrated that they formed a monophyletic group in this order that thrives mainly in volcanic or geothermal environments (Huber and Hannig, 2006) (Fig. 1A). Among these members consisting of two families Fervidobacteriaceae and Thermotogaceae, *F. islandicum* AW-1 together with few strains such as *F. pennivorans* DSM 9078 and *F. thailandense* FC 2004 is distinct in terms of keratin degradation, presumably due to the presence of its protease-rich genome (Lee *et al*., 2015). However, closely related strains of *F. islandicum* AW-1 such as *F. islandicum* H21 and *F. gondwanense* DSM 13020 have been reported to be lacking feather decomposition capability (Nam *et al*., 2002). Although many functional genes are highly conserved in similar strains belonging to this order (Fig. S1A), recent studies on digestion of insoluble feather keratins rich in cysteine suggest that, in addition to proteases (Kang *et al*., 2020), various redox enzymes may play a key role in keratin degradation (Nam *et al*., 2002; Lange *et al*., 2016).

To further investigate the genomic features for these keratin-degrading strains, we performed pan-genomic analysis for these 20 bacterial strains above, revealing that although strains in Thermotogales possess similar levels of genome size, they exhibit a differential gene composition (Fig. S2). Pan-genome analysis provided

© 2020 The Authors. *Microbial Biotechnology* published by Society for Applied Microbiology and John Wiley & Sons Ltd., 

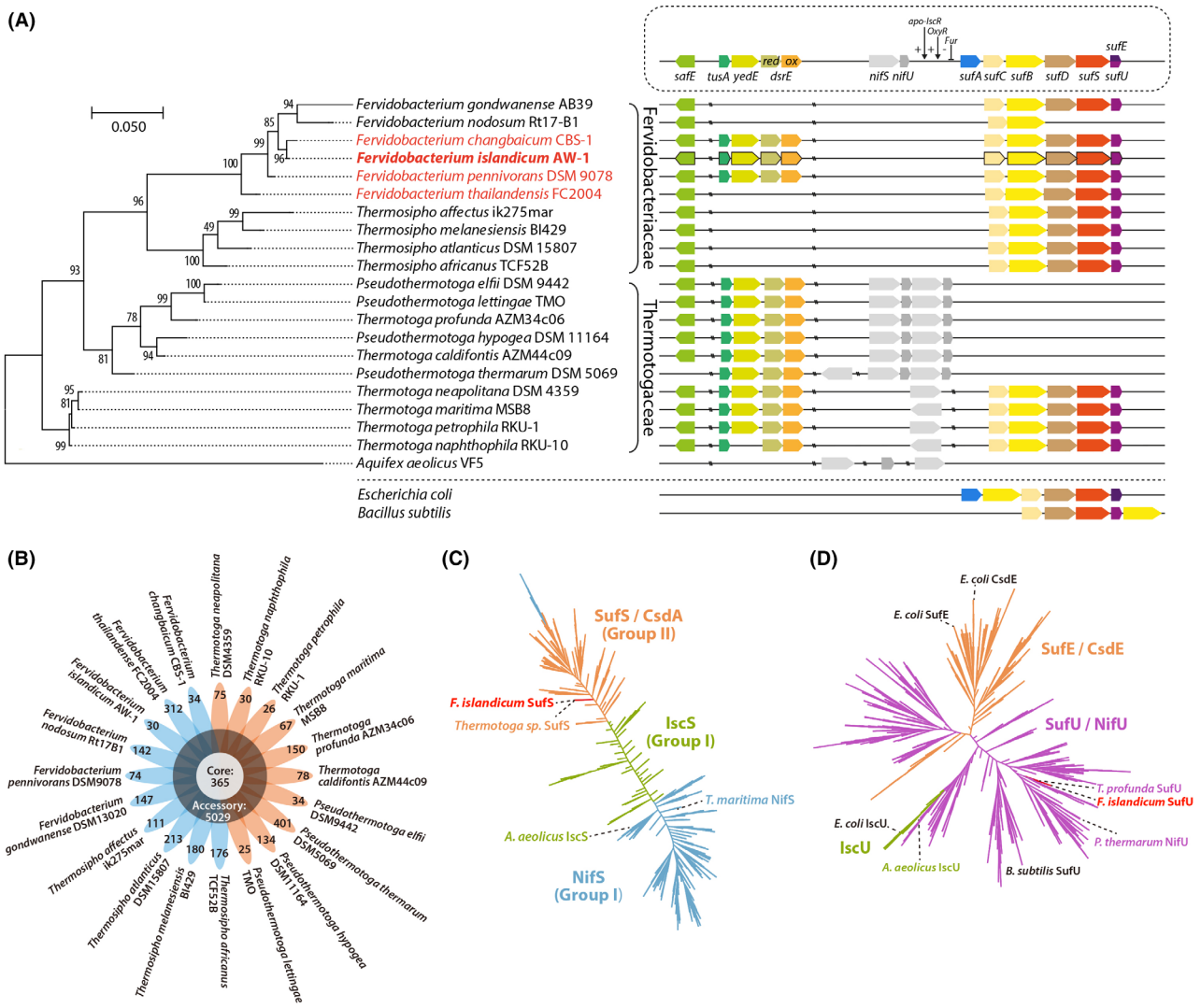


**Fig. 1.** The sulfur formation (Suf) system of the order Thermotogales. A. Phylogenetic analysis based on comparison of 16S rRNA gene sequences of 20 bacterial anaerobes in the order Thermotogales. Phylogeny was inferred using maximum likelihood method and Tamura-Nei model with 1000 bootstrap in MEGA ver. 7.0 program. The scale bar represents the number of changes per nucleotide position. This analysis involved 21 nucleotide sequences including *Aquifex aeolicus* VF5 is used as the out-group and there were a total of 1611 positions in the final data set. Organization of the *suf* operon and putative functional orthologs in the order Thermotogales. Orthologous genes are denoted by the same colour, with the direction of transcription and relative scale indicated by arrows. B. Flower plots showing the core gene number and strain-specific gene number in 20 Thermotogales strains. The number of strain-specific genes per genome is shown in the flower petals. Annotated core and accessory genes are provided in the Table S1, sheet 2. Unrooted phylogenies of (C) cysteine desulfurase (SufS) with its homologues and (D) U-type scaffold protein (SufU) with its functional related homologues of different species. C. Coloured clades contain members of the SufS/CsdA (orange), IscS (green), and NifS (cyan) protein sequences obtained by searching the NCBI Identical Protein Groups database and near-duplicate sequences were removed by UCLUST (Edgar, 2010) clustering to 60% sequence identity. Each tree composed on 2846 representatives of SufS homologues. D. Coloured clades contain members of the SufE/CsdE (orange), IscU (green) and SufU/NifU (purple) protein sequences. Multiple sequence alignments were produced using MAFFT (using its FFT-NS-2) version 7.407 (Katoh and Standley, 2013). Large-scale phylogenetic trees were constructed using raxmlGUI Fast tree search with GAMMA + GTR substitution model. Each tree composed on 3352 representatives of SufU homologues.

the core and variable gene pool among the order Thermotogales (Table S1, sheet 1). The core pan-plot reveals that sequential addition of 20 genomes resulted in the addition of approximately 7833 nonredundant gene families with a plateau (Fig. S1B). This analysis showed that 365 genes constitute the core gene pool of the Thermotogales and that the total variable gene pool comprised more than half of the whole gene pool, or the pan-genome (Fig. 1B). The clustered genes identified for each genome are listed (Table S1, sheet 2). To study the endophenotypic differences, we carried out detailed gene-content analysis, particularly considering the variable or accessory part of the genomes, which was not present in all the strains under study (Table S1, sheet

© 2020 The Authors. *Microbial Biotechnology* published by Society for Applied Microbiology and John Wiley & Sons Ltd., 

2). Overall, the number of unique genes ranged from as low as below 30 in *Pseudothermotoga lettingae* TMO, *Thermotoga petrophila* RKU-1 and *Thermotoga naphthophila* RKU-10 to 401 in *Pseudothermotoga thermarum* DSM 5069 (Fig. 1B). Since their distribution among the phenovars is not uniform, these genes were further annotated and functionally classified using Clusters of Orthologous Groups (COG) classification (Fig. S1C). About two-thirds of total unique genes (66.7%) in the Thermotogales were not assigned to any COG class, suggesting their unveiled roles in the functional diversification of this order. Nevertheless, of 20 COGs, 11 categories including 'Defence mechanisms [V]', 'Inorganic ion transport and metabolism [P]', 'Amino acid transport and metabolism [E]' and 'Function unknown [S]' are dominant among 20 strains in the order Thermotogales with respect to the COG content of unique and accessory genes, which are consistent with KEGG functional categories at a moderate level (Fig. S1D).

The family Fervidobacteriaceae has a relatively lower number of genes belonging to COG class [E], and a higher number of genes belonging to 'post-translational modification, protein turnover and chaperones [O]' than the Thermotogaceae (Fig. S2). On the other hand, the number of genes belonging to [P] is variable. To explore this further, we compared the whole-genome sequence of *F. islandicum* AW-1 with those of its phylogenetically closest relatives in Thermotogales to identify unique genetic features responsible for keratin degradation. We performed pairwise comparisons of functional genes using the Bacterial Pan Genome Analysis tool (BPGA), revealing that strains in the Fervidobacteriaceae possess more functional genes involved in Fe–S cluster assembly, redox-regulated chaperone and the amino acid transporter than the Thermotogaceae (Table S1, sheets 2 to 4). Notably, several genes annotated as cysteine desulfurase (SufS) and SUF system NifU family Fe–S cluster assembly protein (SufU) in the Suf system are absent in the *suf* operon of *F. nodosum* Rt17-B1 (Patel *et al*., 1985) and several Thermotogaceae strains incapable of keratin degradation (Fig. 1A). This distinct feature suggests that the keratinolytic capability of *F. islandicum* AW-1 may be ascribed to the presence of a complete Suf system for Fe–S cluster biogenesis.

### *SufS and SufU from F. islandicum AW-1 exhibit cooperative sulfur transfer activity*

The genome of *F. islandicum* AW-1 (NZ_CP014334) contains the 1266 bp gene NA23_RS08335 and 408 bp gene NA23_RS08330, annotated as SufS family cysteine desulfurase and Suf system NifU family Fe–S cluster assembly protein, respectively. Phylogenetic and sequence similarity analyses revealed that the predicted amino acid sequence of NA23_RS08335 is grouped with SufS/CsdA, sharing high sequence identity with its homologues in *Bacillus subtilis* (*Bs*SufS, 48%) and *E. coli* (*Ec*SufS, 40%) (Figs. 1C and S3A). Analogous studies revealed that NA23_RS08330 belongs to the Nif family protein, sharing high sequence identity with *B. subtilis* SufU (*Bs*SufU, 41%), *Streptococcus pyogenes* NifU (*Sp*NifU, 39%) and *Thermus thermophiles* IscU (*Tt*IscU, 37%), indicating that the NA23_RS08330 is grouped with SufU (Figs. 1D and S3). In addition, their genomic neighbourhood with SufB, C and D indicates clearly that they are part of the Suf-like system. Therefore, we tentatively concluded that these gene products might be *F. islandicum* AW-1 enzymes SufS (*Fi*SufS) and SufU (*Fi*SufU), respectively.

To functionally characterize these proteins, their corresponding genes were expressed in *E. coli* BL21 (DE3). Recombinant *Fi*SufS was yellow in colour, presumably due to the presence of PLP as a cofactor. The apparent molecular masses ($M_r$s) of intact monomeric *Fi*SufS and *Fi*SufU were 47 kDa and 15.5 kDa, respectively (Fig. 2A). The apparent temperature and pH optima of *Fi*SufS were 90°C and pH 8, respectively (Fig. S4A and B). To obtain kinetic parameters for *Fi*SufS, we determined its desulfurase activity by measuring the amount of released sulfide at 90°C and pH 8.0 with cysteine as substrate in the absence of *Fi*SufU, yielding $V_{max}$, $K_m$, and $k_{cat}$ values of 1135.0 $\pm$ 11.0 U/mg, 75.0 $\pm$ 1.7 μM, and 892.7 $\pm$ 8.6 $s^{-1}$, respectively (Fig. 2B). Next, we investigated the effect of *Fi*SufU on *Fi*SufS activity by determining kinetic parameters for *Fi*SufS in the presence and absence of *Fi*SufU. The addition of *Fi*SufU significantly decreased the $K_m$ values for *Fi*SufS by two- to three-fold, resulting in enhancement of SufS activity under reducing conditions (Fig. 2C). This result is consistent with those of previous studies in which SufU interaction with SufS-stimulated desulfurase activity (Outten *et al*., 2003; Selbach *et al*., 2013).

To investigate whether *Fi*SufS and *Fi*SufU can form a complex, we performed size-exclusion chromatography, analytical ultracentrifugation and pull-down assay. Gel filtration data suggested that purified *Fi*SufS and *Fi*SufU were homodimeric and monomeric, respectively (Fig. 2D). Subsequently, both enzymes were mixed and incubated in the presence of 10 mM cysteine and 10 mM DTT at 37°C for 1 h, and reaction mixtures were then subjected to size-exclusion chromatography. The results revealed three major peaks, indicating that the reaction mixtures contained the *Fi*SufS–SufU complex (fractions 14 to 16), as well as dimeric *Fi*SufS (fractions 14 to 16) and monomeric *Fi*SufU (fractions 17 to 19) as judged by SDS-PAGE analysis. Additionally, each fraction was analysed using blue-native (BN)-PAGE, and the observed peak shift to ~ 115.1 kDa further supported the

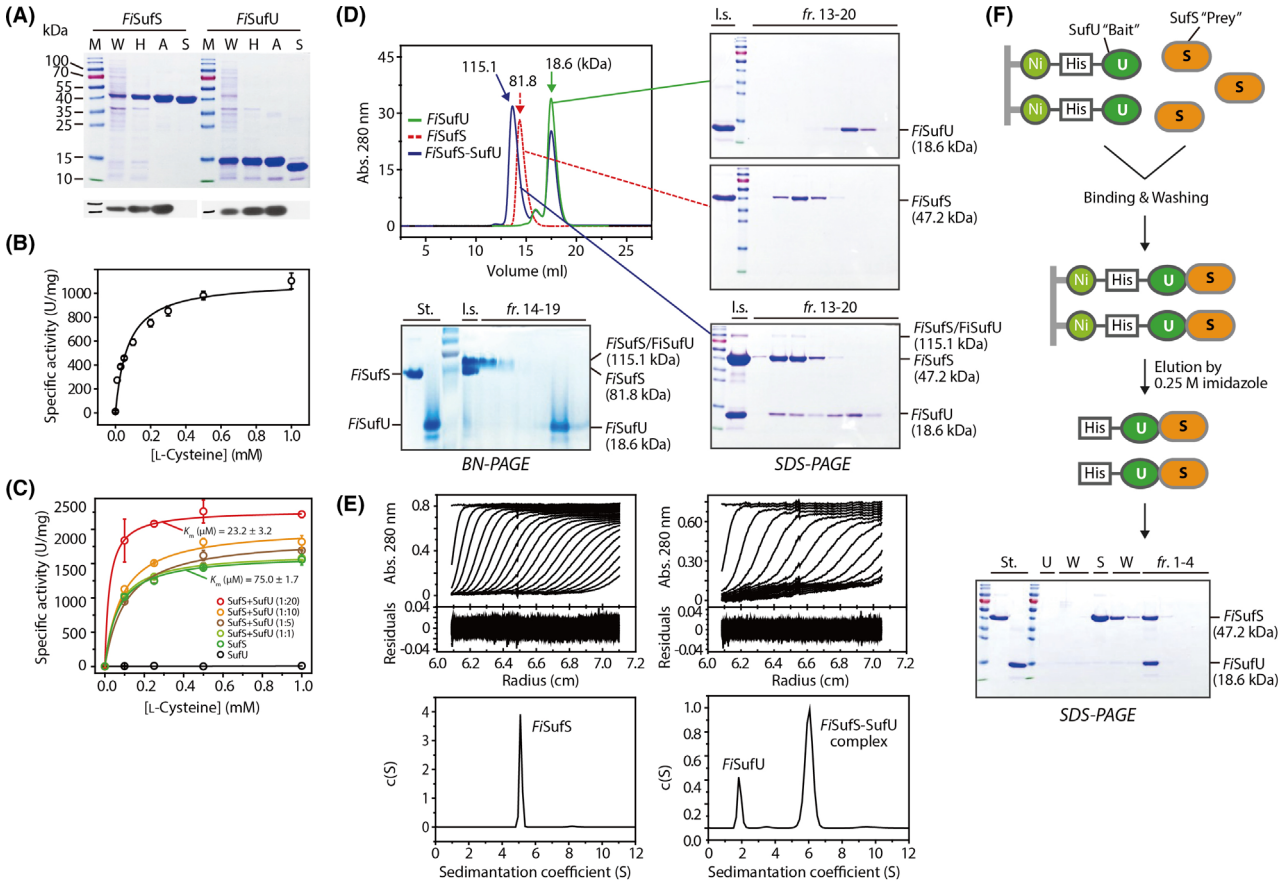


**Fig. 2.** The SufS–SufU complex of *F. islandicum* AW-1. A. SDS-PAGE (top panel) and Western blotting (bottom) analyses of purified *Fi*SufS and *Fi*SufU. Lane 1, molecular weight markers (M); lane 2, whole cell extracts (W); lane 3, heat treatment at 70°C (H); lane 4, $Ni^{2+}$-affinity chromatography (A); lane 5, Superdex 200 chromatography (S). B. Kinetics of recombinant *Fi*SufS. Kinetic parameters could be obtained by fitting experimental data to the Michaelis–Menten (M-M) equation. C. Kinetic analysis of a bisubstrate reaction catalysed by SufS. The lines represent best fits to the M-M equation using Origin 8.0 software. D. Size-exclusion chromatography and electrophoretic analyses of SufS–SufU complex formation. E. Sedimentation velocity analytical ultracentrifugation analysis of *Fi*SufS, *Fi*SufU and the *Fi*SufS–SufU complex. The sedimentation coefficient distribution c(s) shows peaks corresponding to molecular masses. F. Protein–protein interactions between *Fi*SufS and *Fi*SufU assessed by pull-down assays.

formation of the *Fi*SufS–SufU complex (Fig. 2D). Analytical ultracentrifugation (AUC) with the same reaction mixtures above confirmed that the stoichiometric ratio of *Fi*SufS and *Fi*SufU was 2:2 [$(FiSufS)_2$-$(FiSufU)_2$] (Fig. 2E). Lastly, we performed co-purification by loading an excess of tag-free *Fi*SufS onto a $Ni^{2+}$-NTA column pre-loaded with his-tagged *Fi*SufU (Fig. 2F). After removing unbound *Fi*SufS by washing, an equimolar complex of *Fi*SufS and *Fi*SufU was eluted, confirming direct *Fi*SufS–*Fi*SufU interactions.

### *The crystal structure of the FiSufS–SufU complex reveals a specific protein–protein interaction*

The crystal structures of *Fi*SufS, *Fi*SufU and the *Fi*SufS–SufU complex were determined at 2.1 Å, 2.1 Å, and 2.5 Å, respectively (Figs. 3A and S5), and structural details are described in the supplementary information (Table S2, sheet 1). Upon complex formation, *Fi*SufU undergoes several structural changes following binding to *Fi*SufS and sulfur transfer (Fig. 3B and C). Firstly, the two β-sheets (β1 and β2) containing Cys34–S–SH (*Fi*SufU) are decreased significantly in length and transformed into a loop, whereas the length of the Cys34-containing loop between β1 and β2 increases (from $^{31}$NLSCG$^{35}$ to $^{29}$GKNLSCGDEV$^{38}$). This transformation likely renders *Fi*SufU more flexible and therefore better able to receive sulfur from *Fi*SufS. As shown in Fig. 3A and B, the movement of the Cys34-containing loop in *Fi*SufU into the groove of *Fi*SufS by at least 11 Å results in an interatomic distance of 5.5 Å between Cys372–S–SH (*Fi*SufS) and Cys34–S–SH (*Fi*SufU), suggesting that this dynamic Cys34 loop might move even closer to form a disulfide bridge with Cys372–S–SH during sulfur

© 2020 The Authors. *Microbial Biotechnology* published by Society for Applied Microbiology and John Wiley & Sons Ltd., 

transfer (Kato *et al*., 2002). Therefore, our structure may reveal a snapshot of sulfur transfer from persulfurated SufS ($SufS_{per}$) to SufU. Secondly, the $Zn^{2+}$ in the active site of *Fi*SufU appears to be perturbed by the incoming $^{350}$HPH$^{352}$ residues of *Fi*SufS upon binding, resulting in the replacement of Cys34 (*Fi*SufU) with His352 (*Fi*SufS) (Fig. 3A and B). This might facilitate the movement of Cys34 towards Cys372–S–SH (*Fi*SufS), allowing it to receive the sulfur, suggesting that the conserved His352 plays an important role in *Fi*SufU binding and sulfur transfer, as was the case for *Bs*SufS–SufU (Blauenburg *et al*., 2016; Fujishiro *et al*., 2017).

The direct transpersulfuration reaction between SufS and SufU is so instantaneous that the exact snapshot of sulfur transfer still remains unclear. The structure of *Bs*SufS–SufU enables postulation of the mechanism of transpersulfuration between these two proteins (Fujishiro *et al*., 2017). Structural alignments of *Fi*SufS–SufU with *Bs*SufS–SufU revealed that *Bs*SufU in the complex is tilted by 15° away from the binding site of *Fi*SufU with RMSD of 0.836 Å (Fig. S6A and B). Upon closer observation of the side-chain orientations in Cys34–S–SH residues of both SufUs, it might reveal the movement of Cys372–S–SH (*Fi*SufS) and the dissociation of *Fi*SufU from the SufS–SufU complex (Figs. 3B and S6). The Cys34–S–SH side-chains (*Fi*SufU) on both C and D chains in *Fi*SufS–SufU indicate the movement towards *Fi*Cys372–S–SH in SufS for sulfur transfer, and the side-chain of *Bs*Cys41–S–SH leaving towards the hydrophobic pocket in the active site of *Bs*SufU for dissociation (Fujishiro *et al*., 2017). Taken together, we suggest that the structure of *Fi*SufS–SufU complex may reveal a mechanistic snapshot of the sulfur transfer between SufS and SufU, whereas *Bs*SufS-SufU likely provides a snapshot of the dissociation of SufU from the complex. Furthermore, the absence of additional conformational changes in *Bs*SufU upon binding with *Bs*SufS reaffirms our interpretation.

Next, to explore the molecular interactions between *Fi*SufS and *Fi*SufU, we generated *Fi*SufS-Cys372Ala and *Fi*SufU-Cys34Ala mutants to analyse the catalytic role of these residues in sulfur transfer. The addition of a 20-fold molar excess of *Fi*SufU to reaction mixtures resulted in a nearly 2-fold increase in SufS activity in the absence of *Fi*SufU (Fig. 2C). However, equimolar addition of *Fi*SufU-Cys34Ala yielded a significant decrease in enzyme activity compared with addition of *Fi*SufU, clearly indicating that the *Fi*SufS–SufU interactions

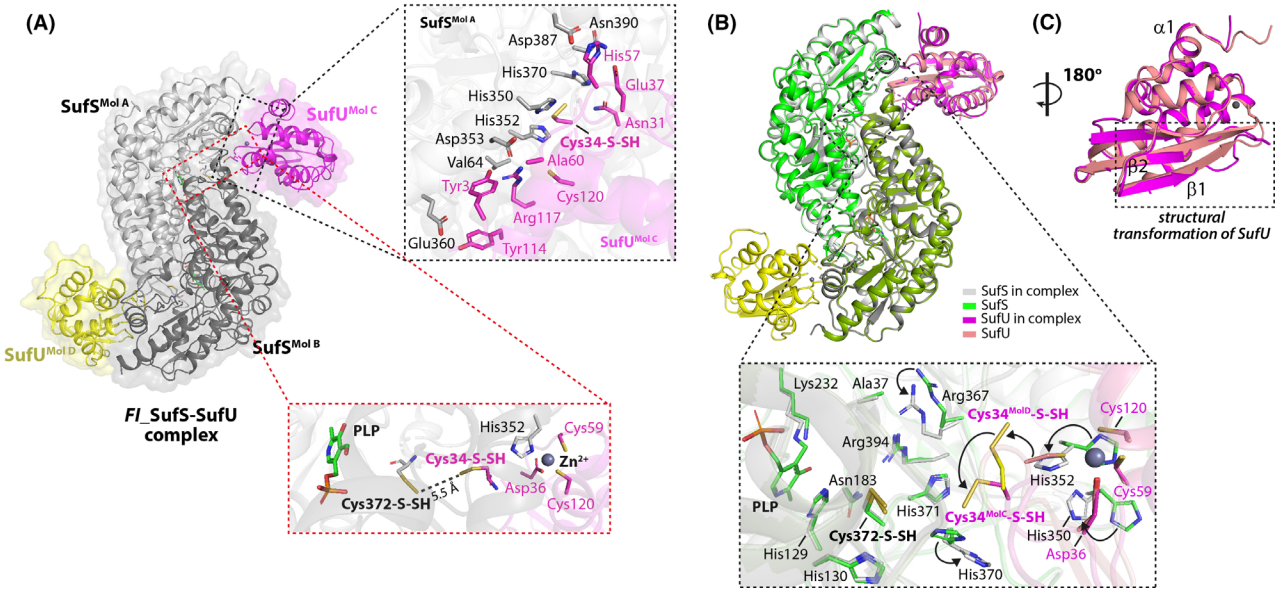


**Fig. 3.** Crystal structure of the *Fi*SufS–SufU complex. A. The *Fi*SufS–SufU complex depicted in ribbon and transparent surface representation. Black dotted box shows the active site. (top panel) Close-up view of the location of the residues of *Fi*SufS and *Fi*SufU in the active site of the complex. Residues of *Fi*SufS alone (green), *Fi*SufU (salmon) and the *Fi*SufS (gray)-SufU (magenta, yellow) complex are represented as sticks. Note the different positions of Cys34–S–SH of *Fi*SufU in chains C (magenta) and D (yellow). Alignment of *Fi*SufU chains C and D reveals a possible movement of *Fi*SufU Cys34–S–SH towards *Fi*SufS Cys372–S–SH during sulfur transfer. A shift in the side-chain of His352 (marked by an arrow) shows that His352 of *Fi*SufS displaces Cys34 in coordination with $Zn^{2+}$ at the *Fi*SufU active site. (bottom panel) Close-up view of the active site, where transpersulfuration reaction is bound to happen between *Fi*SufS and *Fi*SufU. B. Conformational changes in *Fi*SufS and *Fi*SufU upon complex formation. Superimposition of the structures of *Fi*SufS alone (green) and *Fi*SufU alone (salmon) with *Fi*SufS (pale green) bound to *Fi*SufU (magenta). (bottom panel) Close-up view of the active site, depicting the changes in the side-chains of the interface residues upon complex formation. C. Close-up view of the superimposed structures of free *Fi*SufU (salmon) aligned with *Fi*SufU (magenta) in the complex. The major conformational change occurs in the β-sheets, with strands β1 and β2 converted into a loop upon binding to *Fi*SufS.

© 2020 The Authors. *Microbial Biotechnology* published by Society for Applied Microbiology and John Wiley & Sons Ltd., 

involve a sulfane sulfur linkage between the conserved Cys372 (*Fi*SufS) and Cys34 (*Fi*SufU) residues (Fig. S4C). However, complex formation between these two proteins was not affected by these mutations (Fig. S4D).

### *The Suf-like system facilitates decomposition of cysteine-containing keratins*

Unlike other extracellular keratinases from *Bacillus* strains (Lin *et al*., 1995), *F. islandicum* AW-1 has several membrane-bound and cytosolic proteases for keratinolysis (Kang *et al*., 2020). Together with the results above, we presumed that complex keratin degradation exhibits subcellular partitioning of a keratinosome-like protein complex comprising membrane-bound proteases for keratinolysis and unidentified proteins (e.g. the Suf-like system) for sulfitolysis. Thus, we hypothesized that the *Fi*SufS–SufU complex might contribute to generation of the reducing equivalents for cleavage of disulfide bonds during keratin degradation. Since the Suf-like system was minimally expressed in cells grown on glucose compared with cells grown on feathers, we used whole cell extracts from glucose-grown cells (GWCE) as keratinases and investigated whether addition of either *Fi*SufS or *Fi*SufU to GWCE enhanced the rate of feather degradation (Fig. 4A). Thermal incubation at 70°C resulted in minimal degradation of native feathers, regardless of the presence or absence of 10 mM DTT (Fig. 4A), and WCE did not indicate any significant degradation in the absence of DTT (Strasser *et al*., 2015). WCE derived from feather-grown cells (FWCE) exhibited a faster decomposition than GWCE, consistent with previous observations (Jin *et al*., 2017; Kang *et al*., 2020). Furthermore, the decomposition rate was highest when fivefold *Fi*SufU was added, indicating that addition of the *Fi*SufS–SufU complex to GWCE accelerated the feather decomposition rate probably due to the synthesis of $H_2S$ in the presence of DTT, thereby contributing to sulfitolysis (Fig. 4B). This plausible scenario is further supported by recent results that SufS produces $H_2S$ via the persulfide intermediate under anaerobic conditions (Wang *et al*., 2019).

To investigate whether expression of the Suf-like system is activated for feather degradation, we performed qRT-PCR with RNAs extracted from *F. islandicum* AW-1 cells (Fig. 4 and Table S3). Intriguingly, genes encoding peptide/cysteine ATP-binding cassette (ABC) transporters, sulfur formation proteins, together with stress response-related genes encoding DnaK, DnaJ, chaperone Hsp33, and 2-oxoacid:ferredoxin oxidoreductase (OFOR), sulfite exporter TauE/SafE family protein (SafE) were upregulated in cells grown on feathers compared with cells grown on glucose in the absence of elemental sulfur ($S^0$). These results suggest that the Suf system including *Fi*SufS and *Fi*SufU and stress response proteins together with keratinolytic proteases might be required for feather degradation, which was also observed under starvation conditions (Kang *et al*., 2020). Therefore, this result demonstrates that the dissociation of sulfide and sulfane sulfur from cysteine-containing peptides hydrolysed by membrane proteases in WCE may facilitate the disassembly of fibrous keratins through sulfitolysis, indicating a synergistic effect between the *Fi*SufS–SufU complex and membrane and cytosolic proteases.

### *The Suf-like system is coupled to the cystine/cysteine recycling for keratin degradation*

The increased rate of keratinolysis with the *Fi*SufS–SufU complex indicated that cellular sulfur availability might be tightly coordinated with keratin decomposition. To validate the effect of the sulfur source on keratin degradation by *F. islandicum* AW-1, we examined whether keratin digestion is accelerated or retarded when cells are grown in the mTF medium supplemented with feathers in the presence and absence of $S^0$ (Fig. 4). Remarkably, cells grown on feathers with $S^0$ exhibited a higher cellular growth than those without $S^0$ (Fig. 4D). However, feather degradation by *F. islandicum* AW-1 was significantly delayed and their keratin degradation activity was also decreased in the presence of $S^0$ (Fig. 4E–G), indicating that a limitation to cellular sulfur availability is a prerequisite for keratin decomposition. Furthermore, differential expression gene (DEG) analysis of sulfur utilization genes using qRT-PCR supports the notion that the expression of the *suf* operon and sulfur-related genes were significantly upregulated in the absence of $S^0$ (Fig. 4H). Indeed, the genes encoding Suf system, SafE, sulfur relay proteins (i.e. YedE, DsrE and TusA), and stress response-related proteins (e.g. DnaK, Hsp33, and OFOR) were upregulated in cells grown on feathers without $S^0$, whereas genes encoding peptide/cysteine ABC transporters were downregulated in the presence of $S^0$. Taken together, these results suggest that the Suf system including *Fi*SufS and *Fi*SufU and stress response proteins might be required for feather degradation under sulfur starvation conditions.

Although *F. islandicum* AW-1 exhibited a strong keratinolytic activity under starvation conditions, it remains unclear what substances are mainly responsible for generating an extracellular reducing equivalents under starvation conditions, and how insoluble keratins enriched with cysteine disulfide bonds can be utilized as a sulfur source by cells. We assumed that either metabolites and/or cytosolic products by the Suf-like system might be linked to generation of potential redox mediators for sulfitolysis across cellular membranes. To examine this,

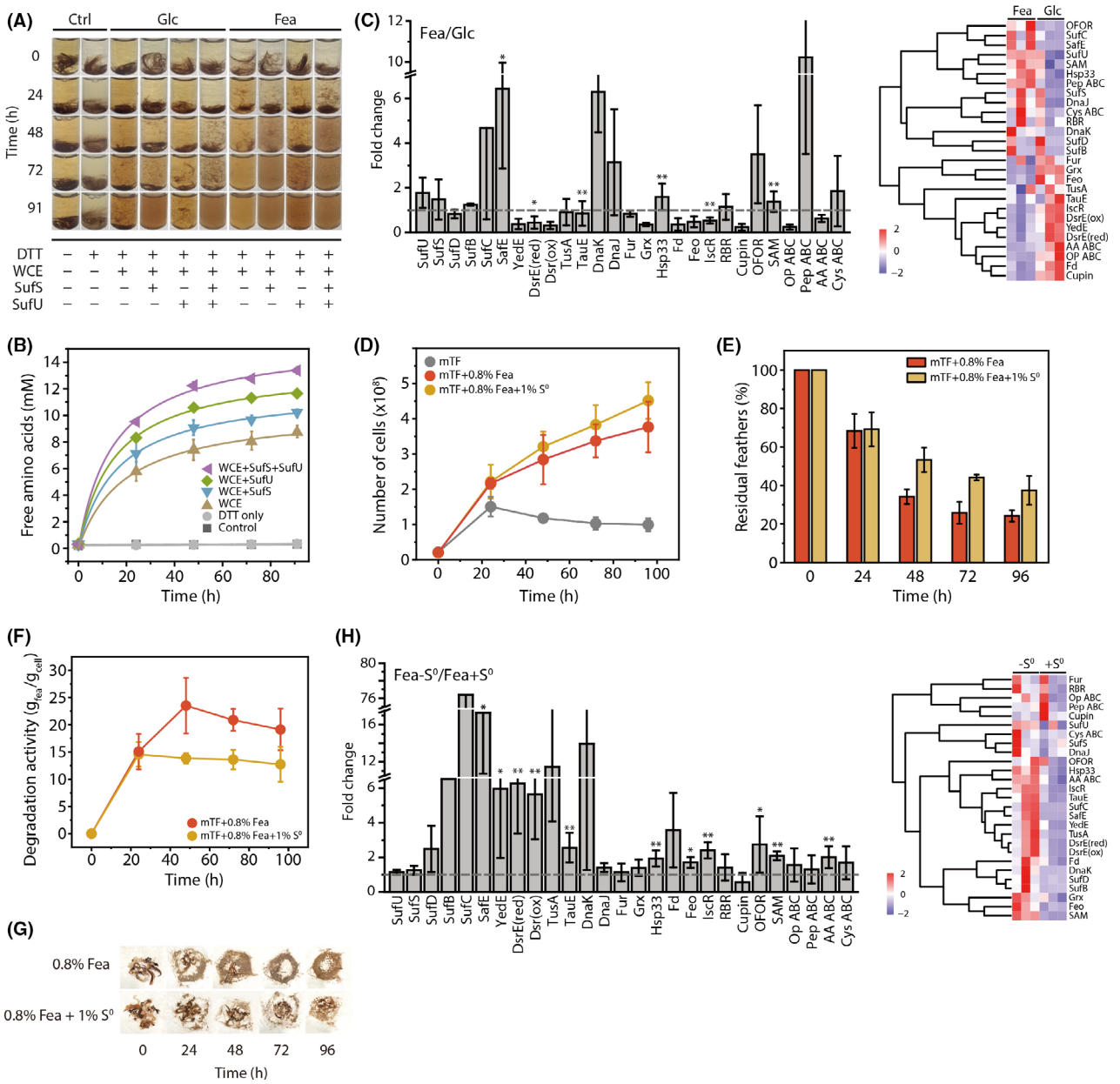


**Fig. 4.** Effects of sulfur availability on the *Fi*SufS–SufU complex-aided keratin degradation. A. The effect of Fe–S assembly proteins on decomposition of native feathers and (B) time-course of free amino acid production by whole cell extracts (WCE) derived from glucose- and feather-grown cells, in the presence and absence of the *Fi*SufS–SufU complex at 80°C. C. Differential expression of genes affecting Fe–S cluster biogenesis in *F. islandicum* AW-1 following growth on glucose and feathers during the mid-exponential growth phase by qRT-PCR analysis. Data were normalized to RpoD expression and fold-change in expression was calculated by the $2^{-\Delta\Delta CT}$ method (Livak and Schmittgen, 2001). Mean ± SD values are plotted and significance was calculated by paired sample *t*-test (*$P < 0.05$, **$P < 0.01$). The heat map shows $\log_2$ expression values. D. Growth curves of *F. islandicum* AW-1 in mTF medium only and mTF medium supplemented with 0.8% feathers in the presence and absence of $S^0$ during anaerobic cultivation at 70°C. E. Time-course of relative residual feathers during anaerobic cultivation with *F. islandicum* AW-1 grown in mTF medium supplemented with 0.8% feathers in the presence and absence of $S^0$. F. Time-course of feather degradation activity (per g cells) during anaerobic cultivation with *F. islandicum* AW-1 grown in mTF medium supplemented with 0.8% feathers in the presence and absence of $S^0$. G. Time-course of feather degradation by *F. islandicum* AW-1 in the presence and absence of $S^0$. H. Differential expression of genes affecting Fe–S cluster biogenesis in *F. islandicum* AW-1 following growth on 0.8% feathers in the presence and absence of $S^0$ during the mid-exponential growth phase by qRT-PCR analysis. Data were normalized to RpoD expression and fold-change in expression was calculated by the $2^{-\Delta\Delta CT}$ method. Mean ± S.D. values are plotted, and significance was calculated by paired sample *t*-test (*$P < 0.05$, **$P < 0.01$).

© 2020 The Authors. *Microbial Biotechnology* published by Society for Applied Microbiology and John Wiley & Sons Ltd., 

we investigated the relative abundance of extracellular and intracellular metabolites using mass spectrometry-based metabolite profiling of cells grown on defined mTF medium containing 0.1% yeast extract supplemented with and without feathers (Fig. 5A). Principal component analysis (PCA) revealed the time-resolved profiles that clearly differed by culture conditions (Fig. S7A). Partial least squares-discriminant analysis (PLS-DA) with random permutation (999 times) demonstrated an appropriate level of statistical significance for the estimated predictability of the model (Figs. 5B and C). Separation between the two groups was mainly explained by t[1], which accounts for the largest degree of variation in the data set, whereas the cultural time-course was largely explained by t[2], the second largest variation. Compositional characteristics were further interrogated with a focus on amino acids. Feather keratin is enriched with hydrophobic amino acids as well as cysteine/cystine (Yeo *et al.*, 2018). Indeed, most hydrophobic amino acids including valine and isoleucine were more abundant in the culture supernatants of cells grown in mTF medium supplemented with feathers than in those of cells in mTF medium containing yeast extracts only (Fig. 5D). Particularly, the extracellular levels of cysteine and cystine as potential redox pairs increased gradually over time during feather degradation for cells grown on feathers, whereas their intracellular concentrations were at equivalent or lower levels in cells grown in mTF medium without feathers (Fig. 5D). Most hydrophilic amino acids displayed similar patterns between intracellular and extracellular matrices, with lower levels in mTF medium containing feathers than in mTF medium alone (Fig. S7B). Although several redox pairs of metabolites, including methionine and methionine sulfoxide, were also detected in the mTF media (Fig. S7C), their production profiles did not correspond to the keratin degradation patterns. Collectively, these results suggest that high levels of extracellular cystine/cysteine coupled to the Suf-like system might contribute to sulfitolysis for keratin degradation. Remarkably, mass spectrometric analysis of extracellular and intracellular levels of amino acids suggested that redox homeostasis within cells coupled to extracellular cysteine and cystine recycling might be a prerequisite for keratinolysis.

## Discussion

Over the last decades, numerous studies on microbial keratin decomposition have been attempted to unveil the molecular mechanism of keratin degradation and elucidate physiological relevance to unusual microbial capability. Nevertheless, it still remains unclear concerning how sulfitolysis can be achieved. In the present study, we performed comparative genomics integrated with comprehensive biochemical and biophysical characterization using an extremely thermophilic *F. islandicum* AW-1 as an excellent model system to investigate the association of the Suf-like system with keratin degradation. Fe–S cluster-containing proteins are primordial, ubiquitous, functionally diverse metalloproteins that are found in all forms of life (Lill, 2009; Netz *et al.*, 2014) (Fig. 1). Since *F. islandicum* AW-1 expresses high levels of *sufCBD* genes on feathers in the absence of $S^0$, we predicted a correlation between sulfur availability and keratin degradation (Figs. 1 and 4), and it is intriguing how SufS and SufU may be involved in the degradation process. Notably, *suf* genes encoding an intact scaffold system for Fe–S cluster biogenesis (i.e. *sufCBDSU*) were upregulated in cells grown on feathers, including sulfite exporter TauE/SafE family protein and peptide ABC transporter were significantly upregulated in the absence of $S^0$ compared to in cells grown on glucose (Fig. 4). This result indicates that these bacterial cells grown on feathers need the uptake and transport of $S^0$ (or $S^{2-}$) directly from cysteine-containing keratins as the sole sulfur source for the biogenesis of Fe–S cluster (Fig. 4A). Indeed, *F. islandicum* AW-1 expresses significantly high levels of the *suf* genes on feathers in the absence of $S^0$. Sulfur relay proteins such as $DsrE_{red/ox}$, YedE, TusA and SafE were also upregulated, which is beneficial for reducing the extracellular environment. In addition, high levels of DnaK and Hsp33 expression in cells grown on feathers appear to be a hallmark of predisposition of sulfur starvation conditions (Fig. 4H). Intriguingly, the expression levels of the *suf* genes correlated with their proximity to the promoter in the *suf* operon. Indeed, the expression levels of the *sufS* and *sufU* genes were relatively marginal than those of the *sufB*, *sufC*, and *sufD* genes, which might be ascribed to either mRNA instability or additional transcriptional regulation due to a putative binding site of transcriptional repressor Fur in the 3'-end region of the *sufD* gene. Although the *suf*S and *suf*U genes were minimally regulated by the presence and absence of feathers or $S^0$, marginal responses of these essential genes are critical for adapting cells to environmental changes (Outten *et al.*, 2004; Albrecht *et al.*, 2010; Roberts *et al.*, 2017). In this regard, a sulfur transfer activity of SufS enhanced by SufU explains how the SufS–SufU complex promotes cellular growth and Fe–S cluster biogenesis despite low levels of expression (Fig. 2C). Specifically, a transient SufS–SufU complex delivers the 'sulfur source' from some cysteines to the SufBCD scaffold for the Fe–S cluster biogenesis. In addition, SufS can release $S^{2-}$, which can be further oxidized to sulfite and released extracellularly, thereby accelerating feather degradation (Fig. 6). Furthermore, the Suf system-related genes, which play an important role in controlling the Fe–S

© 2020 The Authors. *Microbial Biotechnology* published by Society for Applied Microbiology and John Wiley & Sons Ltd., 

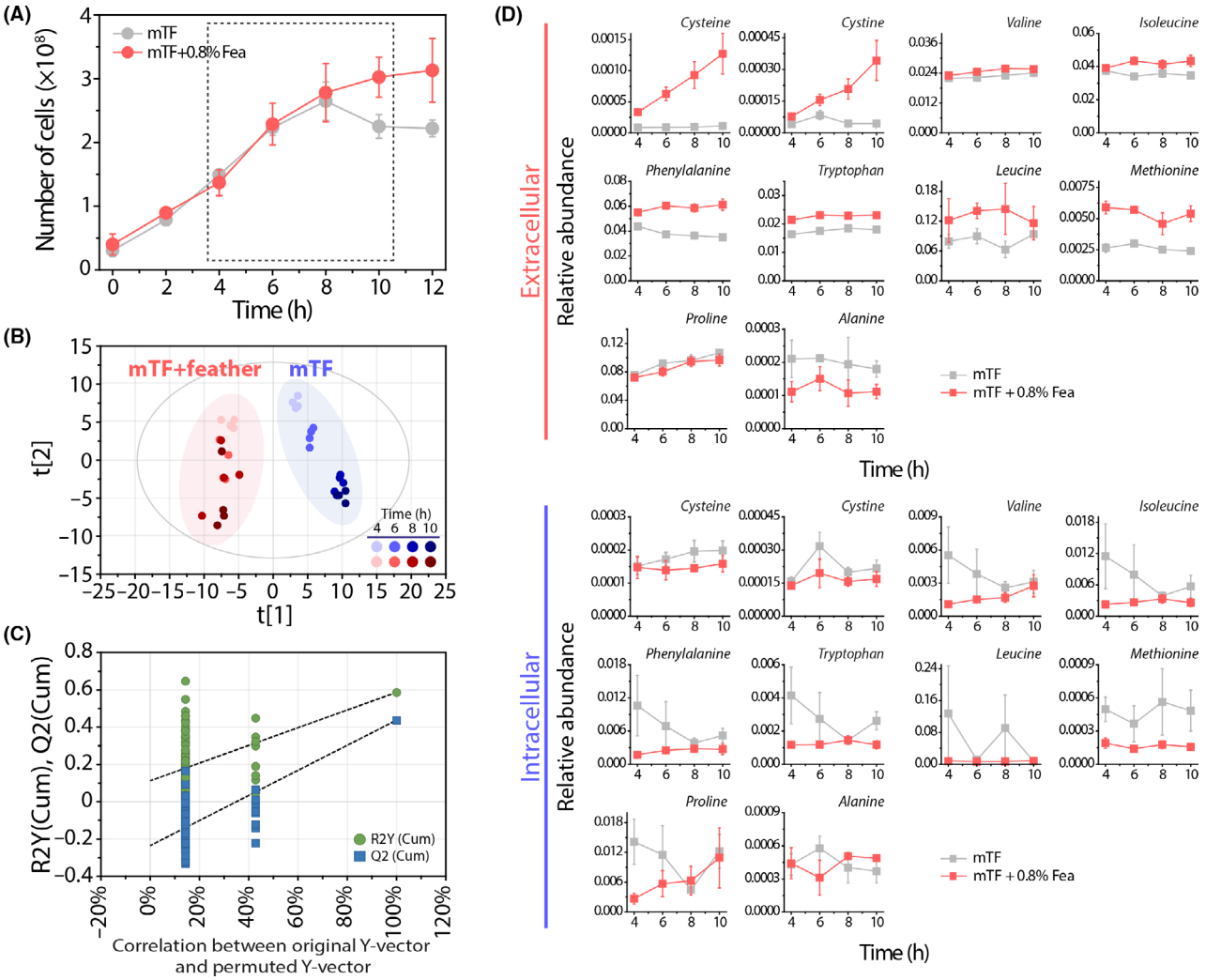


**Fig. 5.** Metabolite profiles of *F. islandicum* AW-1 grown on different nutrients. A. Growth curves of *F. islandicum* AW-1 in mTF medium with and without 0.8% feathers during anaerobic cultivation at 70°C. Dotted lines indicate the sampling time for metabolite analysis. B. Multivariate statistical analysis of extracellular metabolite profiles based on partial least squares-discriminant analysis (PLS-DA). T1 indicates discriminating vector 1 that explains the largest degree of variation in the dataset. Likewise, T2 indicates principal component 2. C. Random permutation plot (999 times) for datasets from the four groups. The vertical axis represents R2Y (green points) and Q2 (blue points) values of the model. The horizontal axis represents the correlation coefficient between original and permuted Y-variables. D. Temporal changes in extracellular and intracellular amino acids in control media (blue line) and media containing feathers (red line). Units are normalized peak height of unique quant mass. Error bars indicate standard error of the mean (SEM).

homeostasis under stress conditions such as iron starvation and oxidative stress, are of importance during the infection cycle of pathogens such as *Dickeya dadantii* (Rincon-Enriquez *et al*., 2008), *Shigella flexneri* (Runyen-Janecky *et al*., 2008) and *Acinetobacter baumannii* (Zimbler *et al*., 2012). Notably, our transcriptomic analysis indicates that expression patterns of *F. islandicum* AW-1 genes related to cellular adhesion to feathers are quite similar to those of these infectious pathogens (J-Y. Kim and J-Y. Sung, unpublished data).

Collectively, the regulation of *suf* genes expression in response to sulfur availability indicates that keratinolysis and Fe–S cluster biogenesis might be tightly coordinated. Therefore, we suggest a plausible mechanism in which cysteine/cystine and peptides, including amino acids released from keratin, are transported into cells, concomitant with the release of sulfur from these cysteines by the *Fi*SufS–SufU complex to support intracellular Fe–S biogenesis. Consequently, the sulfur from SufS can be transferred to the SufBCD system via the SufU as an intermediate cysteine-containing sulfur acceptor between active cysteines in the presence of ferredoxin and Fe–S oxidoreductase for Fe–S assembly (Fig. 6). The sulfur of the intermediate acceptors can be further

© 2020 The Authors. *Microbial Biotechnology* published by Society for Applied Microbiology and John Wiley & Sons Ltd., 

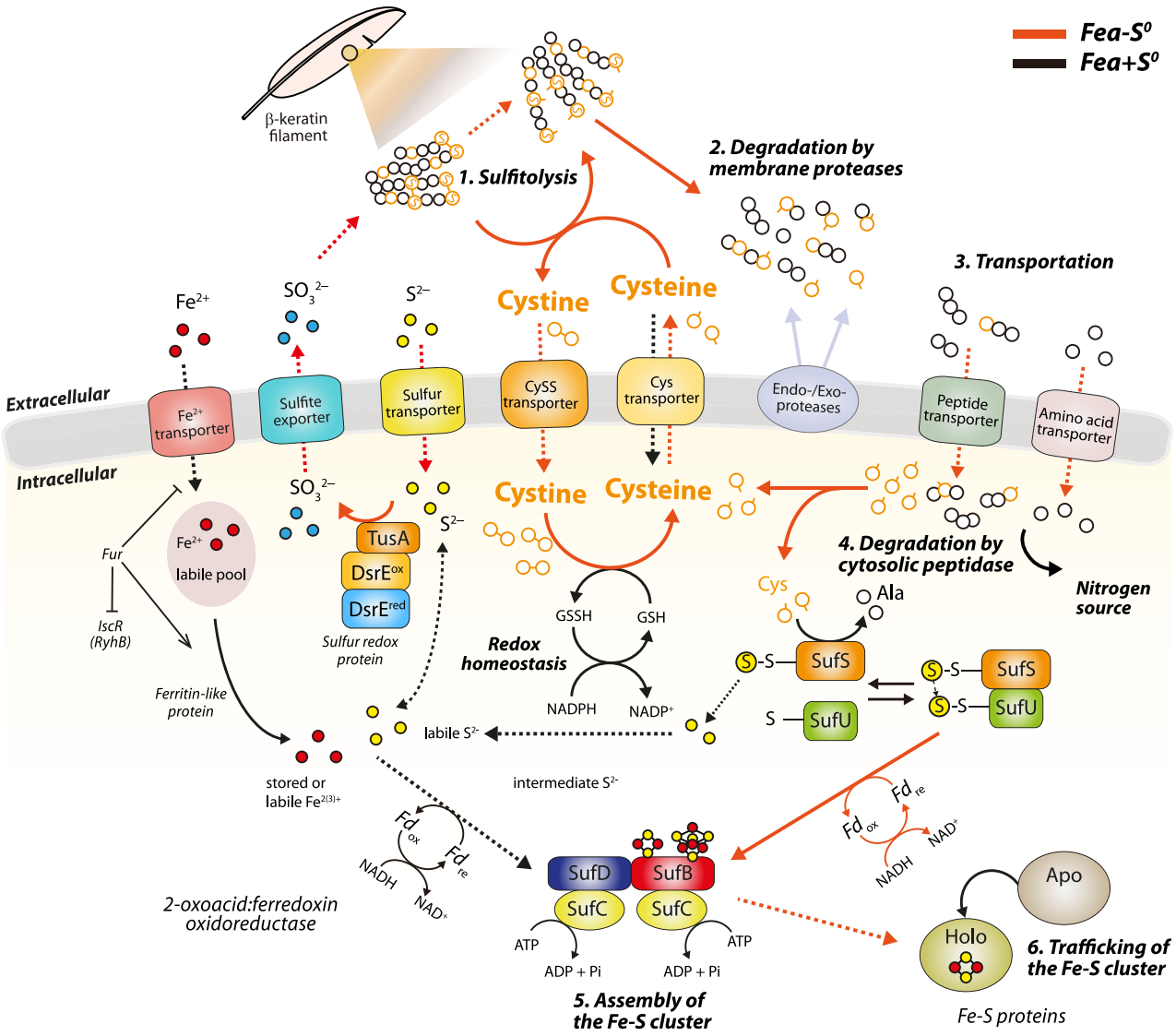


**Fig. 6.** Proposed mechanism of the *Fi*SufS–SufU complex mediating extracellular cysteine and cystine recycling in keratin degradation by *F. islandicum* AW-1. The schematic view shows the proposed role of the Suf system in Fe–S cluster biogenesis and the decomposition of keratin. The cysteine disulfide bonds in recalcitrant keratin structures can be cleaved by extracellular sulfite and/or cysteine as a reducing agent, which makes keratinolysis more feasible by membrane-bound proteases. SufS forms a transient *Fi*SufS–SufU complex to incorporate sulfur sources from cysteines into the Fe–S clusters, and it also releases sulfide to be further oxidized via sulfur redox proteins to sulfite as an extracellular reducing agent. To maintain intracellular levels of L-cysteine below the threshold of cytotoxicity, extra cysteines within cells are excreted to an extracellular environment for maintaining intracellular redox homeostasis based on the ratio of L-cysteine and L-cystine. Consequently, excreted sulfite and cysteines might further facilitate sulfitolysis for keratin degradation. Dotted lines represent the delivery of sulfur sources (persulfurated sulfur and Fe–S clusters), and solid lines indicate enzyme-catalysed reactions.

supplied to Fe–S scaffolds, as well as proteins of sulfur-utilizing pathways such as those involved in the synthesis of sulfur-containing cofactors or thiol modification of tRNA (Takahashi and Tokumoto, 2002; Fontecave and Ollagnier-de-Choudens, 2008). Fe–S cluster-containing proteins are involved in electron transfer, redox catalysis, structure stabilization and sensing functions (Roche *et al.*, 2013; Golinelli-Cohen and Bouton, 2017). Moreover, maintenance of intracellular redox homeostasis results in the release of extra cysteine and cystine from cells, which contributes to the generation of an extracellular reducing environment (Park and Imlay, 2003; Ezraty *et al.*, 2017), thereby facilitating the disassembly of fibrous keratins through the reduction of disulfide bonds heavily cross-linked in feather keratins (Fig. 6). Simultaneously, intracellular cysteine and cystine play a crucial role in cellular redox homeostasis within cells (Ohtsu *et al.*, 2010). Indeed, our metabolomic readout results

© 2020 The Authors. *Microbial Biotechnology* published by Society for Applied Microbiology and John Wiley & Sons Ltd., 

indicate that to maintain intracellular levels of L-cysteine below the threshold of cytotoxicity, surplus L-cysteines are released outside the cell, and this might be involved in chemical reduction of disulfide bonds in keratin (Figs. 5 and 6). Furthermore, the *Fi*SufS–SufU complex mediated the conversion of sulfide derived from L-cysteine and incorporation of iron into Fe–S clusters, which is needed to prevent cellular L-cysteine levels from getting too high during/following keratin degradation. Fe–S cluster-containing proteins can act as rapid and efficient stress response systems, which may help cells to retain crucial activities in response to changes in nutrient including $S^o$ availability, cellular redox potential or other environmental perturbations (Golinelli-Cohen and Bouton, 2017). This explanation is more supported by the growth profiles of *F. islandicum* AW-1 in the presence and absence of $S^0$. As shown in Fig. 4, cellular reproduction was increased in cells grown on feathers in the presence of $S^0$, whereas the capability of keratin degradation (per g cell) was rather decreased, indicating that non-availability of sulfur sources necessitates the stress response, thereby promoting keratin degradation to provide the formation of extracellular free cysteine and cysteine-containing peptides as a sulfur source for the Fe–S biogenesis as well as a nitrogen source for survival. Accordingly, we suggest that SufS and SufU can play an important role in redox homeostasis by modulating the flux of L-cysteine within cells. Primarily, L-cysteine can be desulfurized by SufS, and the resulting sulfane sulfur can be transferred via the SufS–SufU complex to the SufBCD complex for the Fe–S cluster biogenesis (Fig. 6). On the other hand, the excess amounts of intracellular L-cysteine, which can cause intracellular oxidative stress, should be pumped out to extracellular environments by cysteine transporters for maintaining intracellular redox homeostasis. Hence, in the presence of a high concentration of cysteine, the *Fi*SufS–SufU complex in *F. islandicum* AW-1 may be activated not only to incorporate cysteines into Fe–S clusters, but also to release extra cysteines as an extracellular reducing agent for extracellular sulfitolysis. This suggests that the *Fi*SufS–SufU complex enhances keratinolysis by readily utilizing keratin hydrolysates, thereby shifting the equilibrium in the hydrolysis direction (Fig. 6). In this regard, fundamental and multifunctional roles of the Fe–S cluster system could be highlighted beyond its well-known function for Fe–S biogenesis responsible for cellular metabolism. Superficial infections in human skin caused by dermatophytes (Grumbt *et al*., 2013) support this plausible hypothesis since released cysteine can in turn be used as a substrate for sulfite formation, thereby promoting keratin degradation. Moreover, previous investigation of thiol content in thermophilic organisms suggests that they utilize a more oxidizing intracellular environment to take advantage of protein thermostability imparted by disulfide bonds (Heinemann *et al*., 2014). Intriguingly, the Fervidobacteriaceae possess the complete Suf system for Fe–S cluster biogenesis, which is rarely found in the family Thermotogaceae (Fig. 1A). It is noted that extremophiles in the order Thermogales mainly utilized insoluble $S^0$ (transformed into soluble $S^{2-}$ as reducing agent) to produce energy transduction (Huber and Hannig, 2006). Our comparative genomic and DEG data indicated that SufBCD as a major Fe–S cluster assembly system including the SufS–SufU complex together with highly expressed sulfur transport systems including TauE/SafE family proteins as sulfite exporters are responsible for producing a reducing power as well as Fe–S cofactor biogenesis in place of sulfur sources ($S^0$ or $S^{2-}$) (Fig. 4). In the light of this, only when insoluble feather keratins rich in cysteine as the potential sulfur source, strains having SufS and SufU in Fervidobacteriaceae would be advantageous over those in Thermotogaceae for their survival under sulfur starvation conditions.

Overall, we propose that microbial keratin degradation might underlie a strategy for survival under sulfur starvation conditions, implying that strains capable of anaerobic sulfurur metabolism may have evolved the ability to use the Fe–S cluster biogenesis machinery for the utilization of sulfur-containing nutrients as well as a survival strategy under stress conditions.

## Experimental procedures

Detailed information can be found in Supporting information. In addition, bacterial strains and culture conditions, genome sequences, pan-genome analysis, qRT-PCR, cloning, SufS assay, keratin degradation assay, purification of recombinant SufS and SufU and the SufS–SufU complex, AUC, protein crystallization, X-ray data collection and structure determination, refinement and metabolite profiling are described in Supporting information materials and methods.

### *Bioinformatics tools*

The Bacterial Pan Genome Analysis (BPGA) pipeline ver. 1.3 package was used for comparative genomic analysis of twenty strains in the order Thermotogales and clusters of orthologous groups (COG) analysis (Chaudhari *et al*., 2016). For comparative genomics, similarity analysis of genes from microbial genome sequences was performed using the National Center for Biotechnological Information (NCBI) BLAST server and CLgenomics software (Chunlab, Seoul, Korea).

© 2020 The Authors. *Microbial Biotechnology* published by Society for Applied Microbiology and John Wiley & Sons Ltd., 

*Accession numbers*

Structural data are available in the Protein Data Bank (www.pdb.org) under the following accession numbers: *Fi*SufS (PDB 6A6E), *Fi*SufU (PDB 6A6F), and *Fi*SufS–SufU (PDB 6A6G).


## Acknowledgments

We thank staff at beamlines PLS-5C and 7A at the Pohang Light Source (PLS) for technical support during data collection and Jin-Ku Park at Mokpo National University Central Laboratory (MNUCL) for technical support during AUC operation and data collection.

## Funding information

This work was supported by the National Research Foundation of Korea (2017M3A9F3043837 to D.W.L. and 2016R1D1A1B03932717 to S.H.L.) funded by the Ministry of Science, ICT, and Future Planning, by the Strategic Initiative for Microbiomes in Agriculture and Food funded by the Ministry of Agriculture, Food, and Rural Affairs (918012-4 to D.W.L.), Brain Korea 21 (BK21) program (H.S.J and J.Y.S. were fellowship awardees by BK21 program), by the Korea Health Technology R&D project (HP20C0082 to D.W.L.) funded by the Ministry of Health & Welfare, and by the Yonsei University Research Fund of ICB192021 (2019-22-0040).


## Conflict of interest

None of the authors have any financial conflict of interest that might be constructed to influence the results or interpretation of this manuscript.

## Author contributions

H.S.J., I.D., J.Y.S., J.W.L., Y.L., E.M.L., Y.K., D.Y.L., S.H.L. and D.W.L. formulated the research plan, carried out experiments, analysed and interpreted the data and drafted the manuscript. H.S.J., I.D., J.Y.S., D.Y.L., S.H.L. and D.W.L. participated in the design of the study and analysed and interpreted the data. S.H.L., D.Y.L. and D.W.L. conceived, planned and supervised the study.

## References


Albrecht, A.G., Netz, D.J., Miethke, M., Pierik, A.J., Burghaus, O., Peuckert, F., *et al*. (2010) SufU is an essential iron-sulfur cluster scaffold protein in *Bacillus subtilis*. *J Bacteriol* **192:** 1643–1651.

Ayala-Castro, C., Saini, A., and Outten, F.W. (2008) Fe-S cluster assembly pathways in bacteria. *Microbiol Mol Biol Rev* **72:** 110–125.

Blauenburg, B., Mielcarek, A., Altegoer, F., Fage, C.D., Linne, U., Bange, G., and Marahiel, M.A. (2016) Crystal structure of *Bacillus subtilis* cysteine desulfurase SufS and Its dynamic Interaction with frataxin and scaffold protein SufU. *PLoS One* **11:** e0158749.

Chaudhari, N.M., Gupta, V.K., and Dutta, C. (2016) BPGA-an ultra-fast pan-genome analysis pipeline. *Sci Rep* **6:** 24373.

Dai, Y., and Outten, F.W. (2012) The *E. coli* SufS-SufE sulfur transfer system is more resistant to oxidative stress than IscS-IscU. *FEBS Lett* **586:** 4016–4022.

Edgar, R.C. (2010) Search and clustering orders of magnitude faster than BLAST. *Bioinformatics* **26:** 2460–2461.

Ezraty, B., Gennaris, A., Barras, F., and Collet, J.F. (2017) Oxidative stress, protein damage and repair in bacteria. *Nat Rev Microbiol* **15:** 385–396.

Fontecave, M., and Ollagnier-de-Choudens, S. (2008) Iron-sulfur cluster biosynthesis in bacteria: mechanisms of cluster assembly and transfer. *Arch Biochem Biophys* **474:** 226–237.

Fosgerau, K., and Hoffmann, T. (2015) Peptide therapeutics: current status and future directions. *Drug Discov Today* **20:** 122–128.

Fujishiro, T., Terahata, T., Kunichika, K., Yokoyama, N., Maruyama, C., Asai, K., and Takahashi, Y. (2017) Zinc-ligand swapping mediated complex formation and sulfur transfer between SufS and SufU for iron-sulfur cluster biogenesis in *Bacillus subtilis*. *J Am Chem Soc* **139:** 18464–18467.

Golinelli-Cohen, M.-P., and Bouton, C. (2017) Fe-S proteins acting as redox switch: new key actors of cellular adaptive responses. *Curr Chem Biol* **11:** 70–88.

Groussin, M., and Gouy, M. (2011) Adaptation to environmental temperature is a major determinant of molecular evolutionary rates in archaea. *Mol Biol Evol* **28:** 2661–2674.

Grumbt, M., Monod, M., Yamada, T., Hertweck, C., Kunert, J., and Staib, P. (2013) Keratin degradation by dermatophytes relies on cysteine dioxygenase and a sulfite efflux pump. *J Invest Dermatol* **133:** 1550–1555.

Heinemann, J., Hamerly, T., Maaty, W.S., Movahed, N., Steffens, J.D., Reeves, B.D., *et al*. (2014) Expanding the paradigm of thiol redox in the thermophilic root of life. *Biochim Biophys Acta - Gen Subjects* **1840:** 80–85.

Hidese, R., Inoue, T., Imanaka, T., and Fujiwara, S. (2014) Cysteine desulphurase plays an important role in environmental adaptation of the hyperthermophilic archaeon *Thermococcus kodakarensis*. *Mol Microbiol* **93:** 331–345.

Huber, R., and Hannig, M. (2006) Thermotogales. In: *The Prokaryotes: Volume 7: Proteobacteria: Delta, Epsilon Subclass*. Dworkin, M., Falkow, S., Rosenberg, E., Schleifer, K.-H., and Stackebrandt, E. (eds). New York, NY: Springer, New York, 899–922.

Huet, G., Daffé, M., and Saves, I. (2005) Identification of the *Mycobacterium tuberculosis* SUF machinery as the exclusive mycobacterial system of [Fe-S] cluster assembly: evidence for its implication in the pathogen's survival. *J Bacteriol* **187:** 6137–6146.

Jacobson, M.R., Cash, V.L., Weiss, M.C., Laird, N.F., Newton, W.E., and Dean, D.R. (1989) Biochemical and


© 2020 The Authors. *Microbial Biotechnology* published by Society for Applied Microbiology and John Wiley & Sons Ltd., 

genetic analysis of the nifUSVWZM cluster from *Azotobacter vinelandii*. *Mol Gen Genet* **219:** 49–57.

Jin, H.S., Park, S.Y., Kim, K., Lee, Y.J., Nam, G.W., Kang, N.J., and Lee, D.W. (2017) Development of a keratinase activity assay using recombinant chicken feather keratin substrates. *PLoS One* **12:** e0172712.

Johnson, D.C., Dean, D.R., Smith, A.D., and Johnson, M.K. (2005) Structure, function, and formation of biological iron-sulfur clusters. *Annu Rev Biochem* **74:** 247–281.

Kang, E., Jin, H.-S., La, J. W., Sung, J.-Y., Park, S.-Y., Kim, W.-C., and Lee, D.-W. (2020) Identification of keratinases from *Fervidobacterium islandicum* AW-1 using dynamic gene expression profiling. *Microb Biotechnol* **13:** 442–457.

Kang, N.J., Jin, H.-S., Lee, S.-E., Kim, H.J., Koh, H., and Lee, D.-W. (2020) New approaches towards the discovery and evaluation of bioactive peptides from natural resources. *Crit Rev Env Sci Tec* **50:** 72–103.

Kato, S., Mihara, H., Kurihara, T., Takahashi, Y., Tokumoto, U., Yoshimura, T., and Esaki, N. (2002) Cys-328 of IscS and Cys-63 of IscU are the sites of disulfide bridge formation in a covalently bound IscS/IscU complex: implications for the mechanism of iron-sulfur cluster assembly. *Proc Natl Acad Sci USA* **99:** 5948–5952.

Katoh, K., and Standley, D.M. (2013) MAFFT multiple sequence alignment software version 7: improvements in performance and usability. *Mol Biol Evol* **30:** 772–780.

Kessler, D. (2006) Enzymatic activation of sulfur for incorporation into biomolecules in prokaryotes. *FEMS Microbiol Rev* **30:** 825–840.

Lange, L., Huang, Y., and Busk, P.K. (2016) Microbial decomposition of keratin in nature-a new hypothesis of industrial relevance. *Appl Microbiol Biotechnol* **100:** 2083–2096.

Layer, G., Gaddam, S.A., Ayala-Castro, C.N., Ollagnier-de Choudens, S., Lascoux, D., Fontecave, M., and Outten, F.W. (2007) SufE transfers sulfur from SufS to SufB for iron-sulfur cluster assembly. *J Biol Chem* **282:** 13342–13350.

Lee, Y.J., Jeong, H., Park, G.S., Kwak, Y., Lee, S.J., Lee, S.J., *et al*. (2015) Genome sequence of a native-feather degrading extremely thermophilic eubacterium, *Fervidobacterium islandicum* AW-1. *stand. Genomic Sci* **10:** 71.

Lill, R. (2009) Function and biogenesis of iron-sulphur proteins. *Nature* **460:** 831–838.

Lin, X., Kelemen, D.W., Miller, E.S., and Shih, J. (1995) Nucleotide sequence and expression of kerA, the gene encoding a keratinolytic protease of *Bacillus licheniformis* PWD-1. *Appl Environ Microbiol* **61:** 1469–1474.

Liu, Y., Sieprawska-Lupa, M., Whitman, W.B., and White, R.H. (2010) Cysteine is not the sulfur source for iron-sulfur cluster and methionine biosynthesis in the methanogenic archaeon *Methanococcus maripaludis*. *J Biol Chem* **285:** 31923–31929.

Livak, K.J., and Schmittgen, T.D. (2001) Analysis of Relative gene expression data using real-time quantitative PCR and the $2-\Delta\Delta CT$ method. *Methods* **25:** 402–408.

Loiseau, L., Ollagnier-de-Choudens, S., Nachin, L., Fontecave, M., and Barras, F. (2003) Biogenesis of Fe-S cluster by the bacterial Suf system: SufS and SufE form a new type of cysteine desulfurase. *J Biol Chem* **278:** 38352–38359.

Marinoni, E.N., de Oliveira, J.S., Nicolet, Y., Raulfs, E.C., Amara, P., Dean, D.R., and Fontecilla-Camps, J.C. (2012) $(IscS\text{-}IscU)_2$ complex structures provide insights into $Fe_2S_2$ biogenesis and transfer. *Angew Chem Int Ed Engl* **51:** 5439–5442.

Mettert, E.L., and Kiley, P.J. (2015) Fe–S proteins that regulate gene expression. *Biochim Biophys Acta - Mol Cell Res* **1853:** 1284–1293.

Mihara, H., and Esaki, N. (2002) Bacterial cysteine desulfurases: their function and mechanisms. *Appl Microbiol Biotechnol* **60:** 12–23.

Mueller, E.G. (2006) Trafficking in persulfides: delivering sulfur in biosynthetic pathways. *Nat Chem Biol* **2:** 185–194.

Nam, G.W., Lee, D.W., Lee, H.S., Lee, N.J., Kim, B.C., Choe, E.A., *et al*. (2002) Native-feather degradation by *Fervidobacterium islandicum* AW-1, a newly isolated keratinase-producing thermophilic anaerobe. *Arch Microbiol* **178:** 538–547.

Netz, D.J., Mascarenhas, J., Stehling, O., Pierik, A.J., and Lill, R. (2014) Maturation of cytosolic and nuclear iron-sulfur proteins. *Trends Cell Biol* **24:** 303–312.

Ohtsu, I., Wiriyathanawudhiwong, N., Morigasaki, S., Nakatani, T., Kadokura, H., and Takagi, H. (2010) The L-cysteine/L-cystine shuttle system provides reducing equivalents to the periplasm in *Escherichia coli*. *J Biol Chem* **285:** 17479–17487.

Outten, F.W., Djaman, O., and Storz, G. (2004) A suf operon requirement for Fe-S cluster assembly during iron starvation in *Escherichia coli*. *Mol Microbiol* **52:** 861–872.

Outten, F.W., Wood, M.J., Munoz, F.M., and Storz, G. (2003) The SufE protein and the SufBCD complex enhance SufS cysteine desulfurase activity as part of a sulfur transfer pathway for Fe-S cluster assembly in *Escherichia coli*. *J Biol Chem* **278:** 45713–45719.

Park, S., and Imlay, J.A. (2003) High levels of intracellular cysteine promote oxidative DNA damage by driving the fenton reaction. *J Bacteriol* **185:** 1942–1950.

Patel, B., Morgan, H.W., and Daniel, R.M. (1985) *Fervidobacterium nodosum* gen. nov. and spec. nov., a new chemoorganotrophic, caldoactive, anaerobic bacterium. *Arch Microbiol* **141:** 63–69.

Py, B., and Barras, F. (2010) Building Fe-S proteins: bacterial strategies. *Nat Rev Microbiol* **8:** 436–446.

Rees, D.C., and Howard, J.B. (2003) The interface between the biological and inorganic worlds: iron-sulfur metalloclusters. *Science* **300:** 929–931.

Rincon-Enriquez, G., Crété, P., Barras, F., and Py, B. (2008) Biogenesis of Fe/S proteins and pathogenicity: IscR plays a key role in allowing *Erwinia chrysanthemi* to adapt to hostile conditions. *Mol Microbiol* **67:** 1257–1273.

Roberts, C.A., Al-Tameemi, H.M., Mashruwala, A.A., Rosario-Cruz, Z., Chauhan, U., Sause, W.E., *et al*. (2017) The suf iron-sulfur cluster biosynthetic system is essential in *Staphylococcus aureus*, and decreased suf function results in global metabolic defects and reduced survival in human neutrophils. *Infect Immunity* **85.** e00100–17

Roche, B., Aussel, L., Ezraty, B., Mandin, P., Py, B., and Barras, F. (2013) Iron/sulfur proteins biogenesis in prokaryotes: formation, regulation and diversity. *Biochim Biophys Acta* **1827:** 455–469.

© 2020 The Authors. *Microbial Biotechnology* published by Society for Applied Microbiology and John Wiley & Sons Ltd., 

Runyen-Janecky, L., Daugherty, A., Lloyd, B., Wellington, C., Eskandarian, H., and Sagransky, M. (2008) Role and regulation of iron-sulfur cluster biosynthesis genes in *Shigella flexneri* virulence. *Infect Immun* **76:** 1083–1092.

Schwartz, C.J., Djaman, O., Imlay, J.A., and Kiley, P.J. (2000) The cysteine desulfurase, IscS, has a major role in in vivo Fe-S cluster formation in *Escherichia coli*. *Proc Natl Acad Sci USA* **97:** 9009–9014.

Selbach, B.P., Pradhan, P.K., and Dos Santos, P.C. (2013) Protected sulfur transfer reactions by the *Escherichia coli* Suf system. *Biochemistry* **52:** 4089–4096.

Shi, R., Proteau, A., Villarroya, M., Moukadiri, I., Zhang, L., Trempe, J.F., *et al.* (2010) Structural basis for Fe-S cluster assembly and tRNA thiolation mediated by IscS protein-protein interactions. *PLoS Biol.* **8:** e1000354.

Strasser, B., Mlitz, V., Hermann, M., Tschachler, E., and Eckhart, L. (2015) Convergent evolution of cysteine-rich proteins in feathers and hair. *BMC Evol Biol* **15:** 1.

Takahashi, Y., and Tokumoto, U. (2002) A third bacterial system for the assembly of iron-sulfur clusters with homologs in archaea and plastids. *J Biol Chem* **277:** 28380–28383.

Tsiroulnikov, K., Rezai, H., Bonch-Osmolovskaya, E., Nedkov, P., Gousterova, A., Cueff, V., *et al*. (2004) Hydrolysis of the amyloid prion protein and nonpathogenic meat and bone meal by anaerobic thermophilic prokaryotes and *Streptomyces* subspecies. *J Agric Food Chem* **52:** 6353–6360.

Vaccaro, B.J., Clarkson, S.M., Holden, J.F., Lee, D.W., Wu, C.H., Poole Ii, F.L., *et al*. (2017) Biological iron-sulfur storage in a thioferrate-protein nanoparticle. *Nat Commun* **8:** 16110.

Wang, J., Guo, X., Li, H., Qi, H., Qian, J., Yan, S., *et al*. (2019) Hydrogen Sulfide from cysteine desulfurase, Not 3-mercaptopyruvate sulfurtransferase, contributes to sustaining cell growth and bioenergetics in *E. coli* under anaerobic conditions. *Front Microbiol* **10:** 2357.

Yeo, I., Lee, Y.-J., Song, K., Jin, H.-S., Lee, J.-E., Kim, D., *et al*. (2018) Low-molecular weight keratins with anti-skin aging activity produced by anaerobic digestion of poultry feathers with *Fervidobacterium islandicum* AW-1. *J Biotechnol* **271:** 17–25.

Zheng, L., Cash, V.L., Flint, D.H., and Dean, D.R. (1998) Assembly of iron-sulfur clusters. Identification of an iscSUA-hscBA-fdx gene cluster from *Azotobacter vinelandii*. *J Biol Chem* **273:** 13264–13272.

Zheng, L., White, R.H., Cash, V.L., and Dean, D.R. (1994) Mechanism for the desulfurization of L-cysteine catalyzed by the *nifS* gene product. *Biochemistry* **33:** 4714–4720.

Zheng, L., White, R.H., Cash, V.L., Jack, R.F., and Dean, D.R. (1993) Cysteine desulfurase activity indicates a role for NifS in metallocluster biosynthesis. *Proc Natl Acad Sci USA* **90:** 2754–2758.

Zimbler, D.L., Park, T.M., Arivett, B.A., Penwell, W.F., Greer, S.M., Woodruff, T.M., *et al.* (2012) Stress response and virulence functions of the *Acinetobacter baumannii* NfuA Fe-S scaffold protein. *J Bacteriol* **194:** 2884–2893.

## Supporting information

Additional supporting information may be found online in the Supporting Information section at the end of the article.

**Fig. S1**. Pangenomic, phylogenomic and Average Nucleotide Identity (ANI) analyses of representative 20 strains extremophilic bacteria belonging to the order Thermotogales.

**Fig. S2**. Distribution of genome size and genes encoding functional proteins of all 20 strains belonging to the order Thermotogales in selective COGs.

**Fig. S3**. Amino acid sequence alignment of *Fi*SufS (a) and *Fi*SufU (b) with structurally close homologs of different species.

**Fig. S4**. Characterization of *Fi*SufS and *Fi*SufU, and their protein-protein interactions.

**Fig. S5**. Crystal structures of *Fi*SufS and *Fi*SufU.

**Fig. S6**. The location of the residues in the active site of the *Fi*SufS-SufU complex.

**Fig. S7**. Metabolite profiles of *F. islandicum* AW-1 grown on different nutrients.

**Table S1**. Predicted gene content of the Thermotogales pan-genome.

**Table S2**. Statistics for data collection and refinement for *Fi*SufS, *Fi*SufU, and *Fi*SufS-SufU complex.

**Table S3**. List of primers used in this study.

© 2020 The Authors. *Microbial Biotechnology* published by Society for Applied Microbiology and John Wiley & Sons Ltd., 